HHS Public Access

Author manuscript

Nat Commun. Author manuscript; available in PMC 2013 July 01.

Published in final edited form as:

Nat Commun. 2013 ; 4: 1813. doi:10.1038/ncomms2793.

An isoform of retinoid-related orphan receptor β directs differentiation of retinal amacrine and horizontal interneurons

Hong Liu[1], **Soo-Young Kim**[2], **Yulong Fu**[1], **Xuefeng Wu**[1], **Lily Ng**[1], **Anand Swaroop**[2], and **Douglas Forrest**[1]

[1]National Institutes of Health, NIDDK, Laboratory of Endocrinology and Receptor Biology, 10 Center Drive

[2]NEI, Neurobiology, Neurodegeneration and Repair Laboratory, Bethesda, MD 20892-1772, USA

Abstract

Amacrine and horizontal interneurons integrate visual information as it is relayed through the retina from the photoreceptors to the ganglion cells. The early steps that generate these interneuron networks remain unclear. Here we show that a distinct RORβ1 isoform encoded by the retinoid-related orphan nuclear receptor β gene (*Rorb*) is critical for both amacrine and horizontal cell differentiation in mice. A fluorescent protein cassette targeted into *Rorb* revealed RORβ1 as a novel marker of immature amacrine and horizontal cells and of undifferentiated, dividing progenitor cells. RORβ1-deficient mice lose expression of pancreas-specific transcription factor 1a (Ptf1a) but retain forkhead box n4 factor (Foxn4), two early-acting factors necessary for amacrine and horizontal cell generation. RORβ1 and Foxn4 synergistically induce *Ptf1a* expression, suggesting a central role for RORβ1 in a transcriptional hierarchy that directs this interneuron differentiation pathway. Moreover, ectopic RORβ1 expression in neonatal retina promotes amacrine cell differentiation.

Keywords

orphan nuclear receptor; forkhead box transcription factor Foxn4; basic helix-loop-helix factor Ptf1a; neurogenesis; inhibitory interneuron

Introduction

Amacrine and horizontal cells integrate visual information as it is relayed through the retinal layers from the light-sensitive photoreceptors to the ganglion cells that form the optic nerve. Horizontal cells modify synaptic transmission between photoreceptors and bipolar cells

*Corresponding author: Douglas Forrest, Tel. 301 594 6170, Fax 301 451 7848, forrestd@niddk.nih.gov.

Author contributions

H.L. and D.F. designed experiments. H.L., S.-Y.K., Y.F., X.W., L.N., A.S. and D.F. performed experiments and analyzed data. H.L. and D.F. wrote the manuscript.

Competing Financial Interests

The authors declare no competing financial interests.

whereas amacrine cells modify transmission between bipolar and ganglion cells [1]. These inhibitory interneuron networks are critical for visual function but the controls that generate amacrine and horizontal cells are incompletely understood.

The different cell types of the neural retina are derived from multipotent progenitor cells [2–5]. Transcription factors in dividing progenitor cells or in newly post-mitotic precursor cells often determine retinal cell differentiation fates [6–8]. The forkhead box factor Foxn4 and the basic helix-loop-helix (bHLH) factor Ptf1a are required for differentiation of both horizontal and amacrine cells in mice, suggesting that a common transcriptional signal induces the formation of both interneuron classes [9–11]. The nature of this initial stimulus is unclear but Foxn4 expression in progenitor cells is succeeded by Ptf1a expression in post-mitotic precursor cells [9–13], suggesting the involvement of a transcriptional hierarchy. In addition, the homeodomain protein Prox1 is required for horizontal cell differentiation [14] whereas bHLH proteins Neurod1 (Nd1) and Neurod4 (Nd4, or Math3) are required for amacrine cell differentiation [15], suggesting that other controls promote divergence of amacrine and horizontal cell lineages. Other transcription factors of the bHLH [16–18], non-basic HLH [19], homeodomain [20–22] and other families [23–25] further influence diversity in amacrine cell sub-lineages.

The retinoid-related orphan nuclear receptor β gene (*Rorb*, *Nr1f2*) mediates several neurodevelopmental functions. A total *Rorb* deletion impaired circadian behavior, hindlimb motor control [26], opsin induction in cone photoreceptors [27] and differentiation of rod photoreceptors [28]. The means by which developmental genes such as *Rorb* are able to control diverse cellular functions are often unclear. *Rorb* encodes two N-terminal isoforms, RORβ1 and RORβ2, with undefined functions [29].]

Here we report a key role for RORβ1 in amacrine and horizontal cell differentiation. Moreover, RORβ1 and Foxn4 synergistically activate the *Ptf1a* gene, suggesting that cooperation between this orphan receptor isoform and Foxn4 stimulates amacrine and horizontal cell generation.

Results

Differential expression of RORβ1 and RORβ2 isoforms

To investigate specific functions for the isoforms encoded by *Rorb*, we analyzed the expression of RORβ1 and RORβ2 mRNA during retinal development in mice (Figure 1a). RORβ1 mRNA displayed a broad peak between mid-embryonic stages and the first postnatal week. RORβ1 mRNA expression then declined and was maintained at lower levels into adulthood. In contrast, RORβ2 mRNA was first detected at late embryonic stages and displayed a prominent rise over the first postnatal week. These contrasting expression profiles suggested that each isoform mediates specific functions in retinal development with RORβ1 serving a unique role at earlier stages of neurogenesis.

Deletion of the RORβ1 isoform

To determine the role of RORβ1 and to facilitate detection of its expression at the cellular level, we replaced the RORβ1-specific exon with a green fluorescent protein (gfp) cassette

in mice. RORβ1 and RORβ2 are identical in their central DNA binding and C-terminal domains but differ in their N-terminal extensions, consisting of 2 and 13 amino acids, respectively (Figure 1b). RORβ1 and RORβ2 are expressed from distinct promoters upstream of their respective 5′-coding exons in the *Rorb* gene. The gfp cassette was inserted by targeted mutagenesis in embryonic stem cells which were used to generate mice carrying this $Rorb^{1g}$ allele (Figure 1c). Southern blot and genomic sequencing analyses confirmed the structure of the $Rorb^{1g}$ allele.

RORβ1-specific mRNA was undetectable whereas RORβ2-specific mRNA remained intact in the brain and retina of homozygous $Rorb^{1g/1g}$ (1g/1g) mice (Figure 1d). Western blot analyses demonstrated loss of the major RORβ1-specific protein band and retention of the minor, RORβ2-specific band in the retina of 1g/1g embryos (Figure 1e). Heterozygous +/1g mice showed no overt phenotype but 1g/1g mice displayed abnormal gait with exaggerated raising of the hindlimbs similar to that described for $Rorb^{-/-}$ mice lacking all RORβ isoforms [26], indicating that the RORβ1 isoform is critical for hindlimb motor control (Figure 1f).

Retinal expression pattern of $Rorb^{1g}$ allele

RORβ1 expression was traced in +/1g mice which revealed gfp expression in the embryonic retina as well as in the immature cochlea, brainstem, spinal cord and cerebral cortex, shown at embryonic day 15.5 (E15.5) in Figure 1g. In the retina, gfp expression displayed a dynamically changing pattern beginning in neuroblastic cells as early as E11.5. Strong gfp signals were detected in the nascent amacrine cell zones in both the inner nuclear layer (INL) and ganglion cell layer (GCL) during the embryonic and neonatal period when amacrine cells are generated [5](Figure 2a). By postnatal day 7 (P7), gfp was also detected within the inner plexiform synaptic layer in two stratified layers characteristic of the lateral projections of amacrine cells. Developmentally changing but weaker gfp signals were also detected in bipolar neurons, photoreceptors and Muller glia. In general, gfp signals declined after P7 with low levels remaining at older stages, consistent with previous data for *Rorb* mRNA [30,27]. In the embryonic retina, many gfp^+ cells in the outer neuroblastic layer were positive for proliferating cell nuclear antigen (PCNA), a marker of dividing progenitor cells in G1, S and G2 phases of the cell cycle [31] (Figure 2b).

Further analysis co-localized gfp signals with calbindin, a marker of horizontal cells and a sub-population of amacrine cells at late embryonic and neonatal stages (Figure 2c). At early stages, almost all $calbindin^+$ horizontal cell precursors were gfp-positive. By P1, gfp was also detected in most cells that expressed syntaxin, a marker for all amacrine cell types (Figure 2d). During later stages of differentiation, gfp signals declined in both $calbindin^+$ horizontal and $syntaxin^+$ amacrine cells. Thus, the data indicated that RORβ1 was expressed in progenitor cells and subsequently, at enhanced levels in newly-generated horizontal and amacrine cell precursors, followed by declining levels during later development.

$Rorb^{1g/1g}$ mice lack amacrine and horizontal cells

RORβ1-deficient mice displayed a collapsed inner plexiform layer, disorganized outer plexiform layer and a thin inner nuclear layer that was only 3 or 4 soma deep compared to

~6 soma deep in +/+ mice (Figure 3a). These abnormalities reflected loss of horizontal and amacrine cells as demonstrated on retinal flatmounts analyzed for calbindin, a marker of both cell classes (Figure 3b). Ganglion cells were mis-located in the collapsed inner plexiform layer (Figure 3a) but still formed an optic nerve in 1g/1g mice. Other major classes of retinal cells, including bipolar cells, Muller glia, rods and cones were present as indicated by histology and analysis of cell type markers (Supplementary Figure S1).

Analysis of retinal sections (Figure 3c) revealed loss of multiple amacrine cell subtypes in 1g/1g mice as indicated by loss of signals for: (i) γ-aminobutyric acid (GABA) and neuropeptide Y (NPY), markers of GABA-ergic cells, (ii) glycine transporter T1 (GlyT1) and disabled 1 (Dab1), markers of glycinergic cells, (iii) vesicular glutamate transporter 3 (vGlut3) a marker of glutamatergic cells, (iv) choline acetyl transferase (ChAT), a marker of cholinergic cells, (v) tyrosine hydroxylase (TH), a marker of dopaminergic cells, and (vi) calretinin (calr), a marker of ~40% of all amacrine cells of several sub-types. Analysis of pan-amacrine cell markers syntaxin 1 and Pax6 transcription factor confirmed a general depletion of amacrine cell types (Supplementary Figure S1).

Counts of cells expressing representative amacrine (GABA, Dab1, ChAT, TH, calbindin) and horizontal (calbindin) markers revealed that amacrine and horizontal cells were missing from early stages of development in 1g/1g mice (Figure 3d), indicative of a developmental failure to generate these cells rather than a later loss by degeneration.

Expression of gfp was maintained in the retina in 1g/1g embryos, suggesting that progenitors continued to be generated in the absence of RORβ1 (not shown). Indeed, analysis of Bromodeoxyuridine (BrdU) incorporation, an indicator of cell proliferation, revealed comparable numbers of $BrdU^+$ cells in +/+ and 1g/1g mice at E12.5 and P1 (Figure 4a). Previous studies in *Ptf1a*-deficient mice showed that a lack of amacrine and horizontal cells was accompanied by an excess of ganglion cells, suggesting a possible fate switch for progenitors that normally would form amacrine and horizontal cells [10,11]. We similarly observed ~2-fold increased $Brn3a^+$ ganglion cell numbers at embryonic and neonatal ages in 1g/1g mice (Figure 4b, c). During postnatal development, numbers of $Brn3a^+$ cells declined while increased numbers of caspase 3^+ cells were detected in 1g/1g mice, suggesting that excess $Brn3a^+$ cells were subsequently lost by programmed cell death in 1g/1g mice. This phenotype of loss of horizontal and amacrine cells coupled with increased ganglion cell numbers, suggested that RORβ1, like Ptf1a, may influence a pathway with alternative differentiation outcomes of ganglion cell versus amacrine and horizontal cells [10,11].

Loss of transcription factor expression in $Rorb^{1g/1g}$ mice

The developmental stage at which RORβ1 acts relative to Foxn4, Ptf1a and other transcription factors involved in amacrine and horizontal cell differentiation was investigated. *In situ* hybridization detected the presence of Foxn4 but loss of Ptf1a mRNA in 1g/1g mice at E15.5 (Figure 5a). Quantitative PCR (qPCR) analysis demonstrated a normal developmental profile for Foxn4 mRNA levels whereas Ptf1a mRNA was lacking from early stages in 1g/1g mice (Figure 5b). Previously, a partial loss of Nd1 and Nd4 mRNA was reported in *Foxn4*$^{-/-}$ mice at E15 [9,32]. *In situ* hybridization revealed a moderate reduction of Nd1 and Nd4 mRNA signals in 1g/1g embryos (Figure 5a) and qPCR revealed

37 ± 5 % and 45 ± 8 % ($p < 0.001$) deceases of Nd1 and Nd4 mRNA levels, respectively, in 1g/1g embryos at E14.5 (Supplementary Figure S2).

Loss or reduced expression of transcription factors that influence specifically horizontal (Prox1, Lim1) or amacrine (Nr4a2, bHLHb5, Ebf3) sub-lineage differentiation was also detected in 1g/1g mice by *in situ* hybridization, immunohistochemical and qPCR analyses (Figure 5a)(Supplementary Figure S2). These data suggested that RORβ1 acts upstream of Ptf1a but in parallel with Foxn4 at early stages of amacrine and horizontal cell differentiation.

The Ptf1a gene contains an RORβ1-responsive enhancer

The mechanism of regulation of *Ptf1a* expression in the retina is unknown. Thus, loss of *Ptf1a* expression in 1g/1g mice, suggested the hypothesis that RORβ1 induces the *Ptf1a* gene. Given that *Foxn4*$^{-/-}$ mice similarly lacked *Ptf1a* expression [10], we also tested whether RORβ1 and Foxn4 cooperatively induced *Ptf1a*. Previous studies identified a 2.2 kb upstream region and a 12.4 kb downstream region of the *Ptf1a* gene that directed reporter transgene expression in the spinal cord, hindbrain, pancreas and retina in mice [33,34]. We tested conserved fragments from these regions for enhancer function in response to RORβ1 and Foxn4 using a luciferase reporter with a 0.6 kb *Ptf1a* promoter region (Figure 6a). When transfected into 293T cells, a 1.6 kb downstream fragment, or a 0.8 kbsub-domain of this fragment (En0.8), conferred a remarkable ≥90 fold synergistic activation of the reporter in the presence of both RORβ1 and Foxn4 when normalized over basal expression in the absence of added factors ($p < 0.001$). In contrast, RORβ1 and Foxn4 individually gave only 3.3-fold and 5.1-fold activation respectively (Figure 6c, d)(difference for both factors compared to RORβ1 alone $p < 0.001$, or Foxn4 alone $p < 0.001$). In comparison, other enhancer fragments tested, including the upstream 2.2 kb fragment (Pr/En2.2) gave relatively little change in the response to both factors compared to the promoter alone reporter.

The 0.8 kb sub-fragment contained a candidate RORβ1 response element (RORE, 5′-AAACTAGGTTA-3′) related to the 5′-$(A/T)_n$NAGGTCA-3′ consensus [29,27](Figures 6b, e). This RORE was 100% conserved and the surrounding 760 bp sequence was 75% conserved between human and mouse genomes. Mutagenesis of the RORE in the context of En0.8 impaired both the individual response to RORβ1 and the synergistic response to RORβ1 and Foxn4 (each $p<0.001$ compared to wild type Pr/En0.8)(Figure 6c, d). A control mutation 345 bp distant from the RORE interfered minimally with responses to RORβ1 and Foxn4 (not shown). En0.8 also contained two putative elements for Foxn factors based on a core ACGC motif [35,32], located 185 bp upstream (F1) and 125 bp downstream (F2) of the RORE (Figures 6b, e). Of two candidate ACGC motifs in F1, the downstream site and flanking bases was conserved in mouse and human genomes whereas in F2, the most upstream of two candidate motifs was conserved. Individual mutagenesis of ACGC motifs in F1 and in F2 partly reduced the synergistic response to RORβ1 and Foxn4 ($p < 0.001$) whereas combined mutagenesis of RORE, F1 and F2 more severely diminished the response ($p < 0.001$)(Figure 6c).

Direct regulation of the *Ptf1a* gene by RORβ1 and Foxn4 was suggested by DNA binding studies. In an electrophoretic mobility shift assay (EMSA), an oligonucleotide probe representing the RORE in the En0.8 enhancer bound RORβ1 protein obtained by overexpression in 293T cells (Figure 6f). The shifted band was diminished by addition of excess wild type but not mutant competitor oligonucleotides. The shifted band was also supershifted by addition of antibody against RORβ but not by a control immunoglobulin. Also, probes containing the conserved ACGC sequences in F1 and F2 each bound Foxn4 protein in EMSA (Figure 6g). The specific shifted band for each probe was diminished strongly by wild type but weakly by mutant competitor oligonucleotides.

Although the molecular basis of the synergy between RORβ1 and Foxn4 remains unclear, the possibility that RORβ1 and Foxn4 interact physically was investigated by protein pull-down analyses using extracts from 293T cells that overexpress RORβ1 (β1) and histidine-tagged Foxn4 (H.F4)(Figure 6h). Isolation of tagged Foxn4 by nickel chelate chromatography co-selected RORβ1, which was identified by western blot analysis. The co-selected RORβ1 band was specific but relatively weak. However, in EMSA, the addition of both Foxn4 and RORβ1 did not alter the migration of the RORE probe compared to the shift given by RORβ1 alone, indicating that the RORE site did not represent a composite element that bound a dimeric RORβ1/Foxn4 protein complex (not shown). A reciprocal experiment also indicated that F1 or F2 probes did not represent composite DNA binding sites for RORβ1/Foxn4 complexes. The evidence suggests that RORβ1 and Foxn4 primarily bind to their respective DNA elements in the *Ptf1a* gene and only secondarily contact each other.

RORβ1 promotes amacrine cell generation

To determine if RORβ1 stimulates differentiation in a gain of function experiment, a vector expressing RORβ1 from a constitutively active ubiquitin promoter (Ub/RORβ1) was electroporated into the retina of neonatal (P0) mice [36](Figure 7). A co-electroporated plasmid expressing Td Tomato (TdT) allowed identification of electroporated cells. Differentiation outcomes were analyzed at P14, when amacrine and horizontal cell populations normally have been formed and can be identified by their morphology and location in the retinal layers.

Compared to Ub/empty vector, Ub/RORβ1 electroporated into +/+ mice of the CD1 strain yielded large numbers of TdT^+ cells in the amacrine cell zone of the INL with projections typical of amacrine cells in the inner plexiform layer. Many of these TdT^+ cells also expressed markers for amacrine cell types (GABA, calbindin, GlyT1, syntaxin)(Figure 7a, c). However, Ub/RORβ1 yielded few detectable cells in the location of horizontal cells or displaced amacrine cells, probably reflecting limited competence of progenitor cells at the neonatal stage to form some cell types since horizontal cells and a large proportion of amacrine cells have normally been formed by P0 [3,5].

Apart from increased amacrine cell numbers, Ub/RORβ1 gave diminished numbers of $Chx10^+$ bipolar cells and glutamine synthetase $(GS)^+$ Müller glial cells compared to Ub/empty vector (Figure 7c), suggesting that ectopic expression of RORβ1 may inhibit progenitors at P0 from acquiring certain cell fates. Analysis of markers for rods (Nrl), cones (M and S opsin), ganglion cells (Brn3a) and horizontal cells (Lim1) revealed no differences

in response to Ub/RORβ1 or Ub/empty vector. The lack of cells positive for cone, ganglion and horizontal cell markers was consistent with restricted competence of progenitors at P0 to form certain cell types. In summary, ectopic expression of RORβ1 at P0 stimulated amacrine cell differentiation and partly suppressed bipolar and Müller glial cell outcomes.

We also investigated whether RORβ1 can rescue amacrine and horizontal cell differentiation in neonatal RORβ1-deficient mice (Figure 7b, c). Compared to Ub/empty vector, Ub/RORβ1 yielded many TdT^+ amacrine-like cells, including $syntaxin^+$, $GABA^+$, $GlyT1^+$ and $calbindin^+$ cells in the INL with projections in the inner plexiform layer in 1g/1g mice. Ub/RORβ1 also produced TdT^+/$calbindin^+$ cells at the outer zone of the INL with lateral projections in the outer plexiform layer. Although these cells resided in the location of horizontal cells, they probably represented amacrine cells that had failed to align in the amacrine cell zones in the disorganized INL in 1g/1g mice, since horizontal cells are normally produced only during embryogenesis [4]. We also detected GABA, an amacrine cell marker, in TdT^+ cells at this location (not shown). In summary, ectopic over-expression studies indicate that RORβ1 promotes amacrine cell but not horizontal cell differentiation in +/+ or 1g/1g mice at P0.

Discussion

This study indicates that RORβ1 is critical for the differentiation of amacrine and horizontal cells and for the transcriptional induction of Ptf1a, a necessary factor for the generation of both of these classes of interneurons. The synergistic activation of the *Ptf1a* gene by RORβ1 with Foxn4 suggests that a novel cooperation between an orphan nuclear receptor and a forkhead box factor directs a transcriptional pathway for amacrine and horizontal cell differentiation.

We propose a model in which RORβ1 and Foxn4 cooperatively prompt progenitors to commit to form precursors for horizontal and amacrine cell types (Figure 8). A requirement for two factors, rather than only one, may impose stringent selection over which progenitors make this commitment. Consequently, only the requisite cell population may become committed while adequate pools of progenitors are retained for the generation of other retinal cell types. Foxn4 is restricted to dividing progenitors [9] such that the immediate result of RORβ1 and Foxn4 cooperation may be induction of Ptf1a which is transiently expressed in post-mitotic precursor cells for both classes of interneurons [10,11]. In accord with this early role for RORβ1, $Rorb^{1g/1g}$ mice have reduced expression of many later-acting transcription factors involved in terminal differentiation of horizontal and amacrine cell sub-lineages. Unlike Foxn4, RORβ1 continues to be expressed in post-mitotic horizontal and amacrine cells and may possibly also contribute to later maturational events.

Deficiency of either RORβ1 or Foxn4 [9] results in a partial reduction of expression of Nd1 and Nd4, which are required for amacrine but not horizontal cell differentiation [15]. Thus, RORβ1 and Foxn4 may reside upstream of Nd1 and Nd4, although quantification of Nd1 and Nd4 expression in the pertinent cells is difficult to accomplish as these factors are expressed in many retinal cell types in developmentally changing patterns. Conceivably, in

amacrine cell differentiation, Nd1 and Nd4 act upstream of, or in parallel with, Ptf1a because Nd1 and Nd4 expression is unperturbed in *Ptf1a*$^{-/-}$ mice [10,11].

A given transcription factor gene may control diverse neurodevelopmental functions although the basis for this versatility is often unclear. Our evidence indicates that for *Rorb*, such versatility is facilitated by two properties: first, the ability of RORβ proteins to cooperate with other cell-specific factors, such as Foxn4, and secondly, the ability of the gene to express distinct RORβ1 and RORβ2 isoforms in cell-specific patterns.

RORβ isoforms possess specific DNA binding properties but only weak trans-activating functions, such that cooperation with other activators in different cell types can allow the induction of specific target genes. Cooperation between RORβ1 and Foxn4 produces a potent synergistic induction of *Ptf1a* expression. Although the mechanism is unclear at present, the evidence indicates that RORβ1 and Foxn4 each bind to distinct sites within a 350 bp enhancer region in the *Ptf1a* gene. Potentially, the coordinated binding of both factors leads to recruitment of other co-activators or chromatin-activating complexes that stimulate the promoter of the gene. RORβ isoforms also cooperate with Crx homeodomain factor to induce the *Opn1sw* opsin gene in cones [27] and probably also with Otx2 homeodomain factor to induce the *Nrl* gene in rods [28,37,38]. In each case, DNA binding sites exist for both the RORβ isoform and its cooperating factor suggesting that DNA binding by both factors is required for transcriptional enhancement. Cooperative interactions have also been suggested to allow regulation of the activity of orphan receptors that lack known physiological ligands. For example, DNA binding activity by Drosophila Ftzf1 nuclear receptor is regulated by interaction with a homeodomain protein [39].

The differential expression of N-terminal variant isoforms provides a precise means by which a nuclear receptor gene can direct distinct cellular functions. Thus, RORβ1 mediates differentiation of amacrine and horizontal cells and also control of hindlimb movement. The function of the RORβ2 isoform is currently undefined but the contrasting expression profiles of RORβ1 and RORβ2, and the differing phenotypes of mice deleted for RORβ1 or all RORβ isoforms, implicate RORβ2 in photoreceptor differentiation [26–28]. Highly specialized, cell-specific functions have also been described for isoforms encoded by the retinoid-related orphan receptor γ (*Rorg*) and thyroid hormone receptor β (*Thrb*) genes. The RORγt isoform encoded by *Rorg* serves critical functions in inflammatory lymphoid cells [40] whereas the TRβ2 isoform encoded by *Thrb* controls a key step in the differentiation of cone photoreceptors [41].

Materials and Methods

Targeted mutagenesis and retinal electroporation

RORβ1 and RORβ2-specific exons were identified by alignment of mouse genomic and cDNA sequences (accession nos. NM_001043354, NM_146095). Genomic *Rorb* 5′ and 3′ homology arms isolated from ES cell DNA using Phusion polymerase (NewEngland Biolabs) were inserted into a pACN vector carrying a self-excisable neomycin-resistance gene (tACE-Cre-Neo)[42]. An enhanced gfp cDNA replaced the RORβ1-specific exon. Targeted W9.5 ES cell clones were used to generate chimeric mice by K. Kelley at the

Genetics Core Facility, Mount Sinai School of Medicine. Chimeras were crossed with C57BL/6J mice, then *Rorb*$^{+/1g}$ mice intercrossed to generate +/+, +/1g and 1g/1g progeny on a C57BL/6J x 129/Sv background for analysis. The ACN cassette self-excised during germline transmission from male chimeras to yield the *Rorb*^{1g} allele. Genotypes were determined by Southern blot or PCR using as primers: common reverse 5′-GCCTCTTCTACCCAAAGTCAC-3′, wild type forward 5′-TCATGCGAGGTAAGCGAGC-3′, mutant forward 5′-CAACTACAACAGCCACAACG-3′, yielding wild type and mutant bands of 358 and 653 bp, respectively. *In vivo* electroporation was performed as described [36] in wild type CD1 or *Rorb*1$^{g/1g}$ pups on the mixed background noted above. RORβ1 and Foxn4 cDNAs were inserted into a Ub expression vector [43]. Animal experiments were performed in accordance with protocols approved by the Animal Care and Use Committee at NIDDK and NEI at the National Institutes of Health.

Quantitative PCR (qPCR) and western blot analysis

RNA from pooled retinas (>4 mice/pool) was subjected to reverse transcription and real-time qPCR with normalization to β-actin mRNA levels [28] using primers for Foxn4, Ptf1a, Nd1 Nd4, Lim1, Brn3b, Barhl2, Ebf3, bHLHb5 and Nr4a2 (Supplementary Table S2). Developmental analysis of RORβ1 and RORβ2 mRNA levels (Figure 1a) was determined in triplicate on retinal RNA samples pooled from >3 mice at each age using primers as follows: β1F, 5′-CCATCAGAAACAGTCATCAGCAAC-3′, β1R 5′-TGGGCAGGAGTAAGAGGCATTG-3′, β2F, 5′-CCGTCAGAATGTGTGAGAACCAG-3′, β2R 5′-ATCCTCCCGAACTTTACAGCATC-3′. Samples represented dissected retina except at E13.5, at which age whole eye was used. Western blot analysis was performed on 10 or 20 μg samples of retinal proteins using antibodies for RORβ (rabbit polyclonal, 1/1000, Diagenode pAbRORbHS100) and actin (mouse monoclonal, 1/5000, Millipore MAb1501) with chemiluminescent detection [44].

In situ hybridization and immunohistochemistry

Digoxigenin-labeled antisense and sense riboprobes were used for *in situ* hybridization on 10 μm retinal cryosections with colorigenic detection as described [44]. For immunostaining, 10 μm cryosections were incubated overnight with primary antibody at 4°C, then incubated with fluorescent-conjugated second antibody for 1 hour at room temperature, gently washed 3 times in 1xPBS before addition of mounting medium. Antibodies and dilutions are listed in Supplementary Table S1. Double analysis for gfp and PCNA (or bromodeoxyuridine, BrdU) required pre-treatment of sections in 2M HCl at room temperature for 10 minutes, followed by neutralization in 0.1 M sodium borate buffer for 10 minutes before addition of antibody against PCNA or BrdU. For flatmounts, the eye was fixed in 4% PFA at 4°C for 1 hr. The cornea, lens and pigmented epithelium were removed, then the retinal cup incubated with antibody in blocking buffer for 2–3 days at 4°C, washed several times in PBS for 6 hr, then incubated with second fluorescent antibody for 1 day. The retina was washed in PBS for 2 hr, cut peripherally with 3–5 incisions then flattened on a slide. For BrdU labeling, pregnant female mice or neonatal pups were injected intraperitoneally with 20 μg BrdU/g weight from a 10 μg/μl stock solution 1 hour before eye dissection. For

immunofluorescence, a Leica laser scanning confocal microscope analyzed 0.5 μm planar images stacked to a total 4 μm thickness for retinal flatmounts or sections of electroporated retinas, or a single 0.5 μm plane for other sections. Image brightness and contrast were adjusted using ImageJ (NIH, Bethesda, MD). Cell count data represent means ± s.d.. Statistical analyses of cell counts were performed using Student's two-tailed t-test to compare 1g/1g versus +/+ samples, or test versus control samples in electroporation experiments. For histology, 3 μm methacrylate plastic sections near the vertical mid-line of the eye were stained with hematoxylin and eosin [44].

Reporter plasmid constructs and luciferase assays

Ptf1a promoter and enhancer fragments from C57BL/6J mouse DNA were inserted into pREP4 luciferase reporter vector. Mutations were introduced by site-directed mutagenesis into the reporter vectors using oligonucleotides to change the RORE, F1 and F2 Foxn response elements as follows (changed bases in bold and italics within the underlined core motifs): RORE-mutation 5′-GGGTCTGAAACT***GAA***TT***C***AAGCGATTAGCA-3′; F1 mutation 5′-GAGC***TA***GGGGTTGGGGCAGGAG***CA***GCTC-3′; F2 mutation 5′-AC***GGAT***TGAGATTCTGGGTCGCG***T***CGCTC-3′. Note that for F1 and F2 elements, both candidate Foxn response motifs (ACGC) were changed in each element. Mouse RORβ1 and Foxn4 cDNAs were expressed from pSG5 or pCDNA3.1 vectors transfected into 293T cells in 24 well plates in mixtures containing 100 ng reporter, 5 ng pSV-RL renilla control plasmid, 400 ng expression plasmid and carrier DNA to a total of 800 ng DNA with 2 μl Fugene HD reagent (Roche). Luciferase activity was measured 48 hour after transfection. Samples were analyzed in triplicate and each experiment was repeated three times. Data represent mean ± s.d. Statistical analysis was performed by Student's t-test under different categories: [i] basal activity of each reporter in the absence of added factors was compared individually to promoter alone (Pr) reporter, to rule out basal variations that could distort subsequent analyses of induction; none was significantly different from Pr alone ($p>0.26$); [ii] for determination of the synergistic response of each reporter, the normalized fold induction in the presence of both RORβ1 and Foxn4 was compared to that in the absence of factors or in the presence of only RORβ1 or Foxn4; [iii] to determine the activity of each enhancer fragment, the fold induction of each reporter in the presence of both factors was compared to that of promoter alone (Pr) in the presence of both factors; [iv] to assess the result of mutagenesis of RORE, F1 or F2 in the context of Pr/En0.8, the fold induction over basal level of each mutation construct in the presence of RORβ1 and Foxn4 was compared to the fold induction of wild type Pr/En0.8 in the presence of RORβ1 and Foxn4.

EMSA and protein co-selection analyses

EMSA was performed with 2 μg of nuclear protein extract from transfected 293T cells and 0.2 pmol of ^{32}[P] end-labeled probe as described [27]. Antibody against RORβ or control IgG was pre-incubated with protein at 4°C for 30 min before addition of probe, then incubated at room temperature for 15 min. Competitor probe was added at 5 or 50-fold excess. For protein pull-down studies, extracts from 293T cells transfected with RORβ1 and His_6-Foxn4 expression plasmids were incubated with Ni-beads for 2 hour at 4°C [27]. The histidine tag was fused onto the C-terminus of Foxn4. Proteins were released by heating at 95°C then analyzed by electrophoresis and western blot.

Supplementary Material

Refer to Web version on PubMed Central for supplementary material.

Acknowledgments

We thank C. Stewart for W9.5 ES cells, M. Capecchi for plasmid pACN, D. Kim, T. Badea and M. Ma for advice and assistance and K. Kelley for blastocyst injections. This work was supported by the NIDDK and NEI intramural research programs at the NIH and a grant from the KaroBio Foundation.

References

1. Masland RH. The fundamental plan of the retina. Nat Neurosci. 2001; 4:877–886. [PubMed: 11528418]
2. Sidman, RL. The structure of the eye. Smelser, GK., editor. Academic Press; 1961. p. 487-506.
3. Hinds JW, Hinds PL. Development of retinal amacrine cells in the mouse embryo: evidence for two modes of formation. J Comp Neurol. 1983; 213:1–23. [PubMed: 6826785]
4. Young RW. Cell differentiation in the retina of the mouse. Anat Rec. 1985; 212:199–205. [PubMed: 3842042]
5. Voinescu PE, Kay JN, Sanes JR. Birthdays of retinal amacrine cell subtypes are systematically related to their molecular identity and soma position. J Comp Neurol. 2009; 517:737–750. [PubMed: 19827163]
6. Livesey FJ, Cepko CL. Vertebrate neural cell-fate determination: lessons from the retina. Nat Rev Neurosci. 2001; 2:109–118. [PubMed: 11252990]
7. Brzezinski, J.; Reh, TA. Encyclopedia of the eye. Elsevier; 2010. p. 73-80.
8. Swaroop A, Kim D, Forrest D. Transcriptional regulation of photoreceptor development and homeostasis in the mammalian retina. Nat Rev Neurosci. 2010; 11:563–576. [PubMed: 20648062]
9. Li S, et al. Foxn4 controls the genesis of amacrine and horizontal cells by retinal progenitors. Neuron. 2004; 43:795–807. [PubMed: 15363391]
10. Fujitani Y, et al. Ptf1a determines horizontal and amacrine cell fates during mouse retinal development. Development. 2006; 133:4439–4450. [PubMed: 17075007]
11. Nakhai H, et al. Ptf1a is essential for the differentiation of GABAergic and glycinergic amacrine cells and horizontal cells in the mouse retina. Development. 2007; 134:1151–1160. [PubMed: 17301087]
12. Boije H, Edqvist PH, Hallbook F. Temporal and spatial expression of transcription factors FoxN4, Ptf1a, Prox1, Isl1 and Lim1 mRNA in the developing chick retina. Gene Expr Patterns. 2008; 8:117–123. [PubMed: 18006384]
13. Jusuf PR, Harris WA. Ptf1a is expressed transiently in all types of amacrine cells in the embryonic zebrafish retina. Neural Dev. 2009; 4:34. [PubMed: 19732413]
14. Dyer MA, Livesey FJ, Cepko CL, Oliver G. Prox1 function controls progenitor cell proliferation and horizontal cell genesis in the mammalian retina. Nat Genet. 2003; 34:53–58. [PubMed: 12692551]
15. Inoue T, et al. Math3 and NeuroD regulate amacrine cell fate specification in the retina. Development. 2002; 129:831–842. [PubMed: 11861467]
16. Feng L, et al. Requirement for Bhlhb5 in the specification of amacrine and cone bipolar subtypes in mouse retina. Development. 2006; 133:4815–4825. [PubMed: 17092954]
17. Cherry TJ, et al. NeuroD factors regulate cell fate and neurite stratification in the developing retina. J Neurosci. 2011; 31:7365–7379. [PubMed: 21593321]
18. Kay JN, Voinescu PE, Chu MW, Sanes JR. Neurod6 expression defines new retinal amacrine cell subtypes and regulates their fate. Nat Neurosci. 2011; 14:965–972. [PubMed: 21743471]
19. Jin K, Jiang H, Mo Z, Xiang M. Early B-cell factors are required for specifying multiple retinal cell types and subtypes from postmitotic precursors. J Neurosci. 2010; 30:11902–11916. [PubMed: 20826655]

20. Mo Z, Li S, Yang X, Xiang M. Role of the Barhl2 homeobox gene in the specification of glycinergic amacrine cells. Development. 2004; 131:1607–1618. [PubMed: 14998930]
21. Elshatory Y, et al. Islet-1 controls the differentiation of retinal bipolar and cholinergic amacrine cells. J Neurosci. 2007; 27:12707–12720. [PubMed: 18003851]
22. Ding Q, et al. BARHL2 differentially regulates the development of retinal amacrine and ganglion neurons. J Neurosci. 2009; 29:3992–4003. [PubMed: 19339595]
23. Chen D, et al. Rb-Mediated Neuronal Differentiation through Cell-Cycle-Independent Regulation of E2f3a. PLoS Biol. 2007; 5:e179. [PubMed: 17608565]
24. Cherry TJ, Trimarchi JM, Stadler MB, Cepko CL. Development and diversification of retinal amacrine interneurons at single cell resolution. Proc Natl Acad Sci U S A. 2009; 106:9495–9500. [PubMed: 19470466]
25. Jiang H, Xiang M. Subtype specification of GABAergic amacrine cells by the orphan nuclear receptor Nr4a2/Nurr1. J Neurosci. 2009; 29:10449–10459. [PubMed: 19692620]
26. Andre E, et al. Disruption of retinoid-related orphan receptor β changes circadian behavior, causes retinal degeneration and leads to vacillans phenotype in mice. EMBO J. 1998; 17:3867–3877. [PubMed: 9670004]
27. Srinivas M, Ng L, Liu H, Jia L, Forrest D. Activation of the blue opsin gene in cone photoreceptor development by retinoid-related orphan receptor β. Mol Endocrinol. 2006; 20:1728–1741. [PubMed: 16574740]
28. Jia L, et al. Retinoid-related orphan nuclear receptor RORβ is an early-acting factor in rod photoreceptor development. Proc Natl Acad Sci USA. 2009; 106:17534–17539. [PubMed: 19805139]
29. Andre E, Gawlas K, Becker-Andre M. A novel isoform of the orphan nuclear receptor RORβ is specifically expressed in pineal gland and retina. Gene. 1998; 216:277–283. [PubMed: 9729429]
30. Chow L, Levine EM, Reh TA. The nuclear receptor transcription factor, retinoid-related orphan receptor β, regulates retinal progenitor proliferation. Mech Dev. 1998; 77:149–164. [PubMed: 9831642]
31. Barton KM, Levine EM. Expression patterns and cell cycle profiles of PCNA, MCM6, cyclin D1, cyclin A2, cyclin B1, and phosphorylated histone H3 in the developing mouse retina. Dev Dyn. 2008; 237:672–682. [PubMed: 18265020]
32. Luo H, et al. Forkhead box N4 (Foxn4) activates Dll4-Notch signaling to suppress photoreceptor cell fates of early retinal progenitors. Proc Natl Acad Sci U S A. 2012; 109:E553–562. [PubMed: 22323600]
33. Masui T, et al. Transcriptional autoregulation controls pancreatic Ptf1a expression during development and adulthood. Mol Cell Biol. 2008; 28:5458–5468. [PubMed: 18606784]
34. Meredith DM, Masui T, Swift GH, MacDonald RJ, Johnson JE. Multiple transcriptional mechanisms control Ptf1a levels during neural development including autoregulation by the PTF1-J complex. J Neurosci. 2009; 29:11139–11148. [PubMed: 19741120]
35. Schlake T, Schorpp M, Nehls M, Boehm T. The nude gene encodes a sequence-specific DNA binding protein with homologs in organisms that lack an anticipatory immune system. Proc Natl Acad Sci U S A. 1997; 94:3842–3847. [PubMed: 9108066]
36. Matsuda T, Cepko CL. Analysis of gene function in the retina. Methods Mol Biol. 2008; 423:259–278. [PubMed: 18370205]
37. Kautzmann MA, Kim DS, Felder-Schmittbuhl MP, Swaroop A. Combinatorial regulation of photoreceptor differentiation factor, neural retina leucine zipper gene NRL, revealed by in vivo promoter analysis. J Biol Chem. 2011; 286:28247–28255. [PubMed: 21673114]
38. Montana CL, et al. Transcriptional regulation of neural retina leucine zipper (Nrl), a photoreceptor cell fate determinant. J Biol Chem. 2011; 286:36921–36931. [PubMed: 21865162]
39. Yu Y, et al. The nuclear hormone receptor Ftz-F1 is a cofactor for the Drosophila homeodomain protein Ftz. Nature. 1997; 385:552–555. [PubMed: 9020364]
40. Eberl G, et al. An essential function for the nuclear receptor RORgamma(t) in the generation of fetal lymphoid tissue inducer cells. Nat Immunol. 2004; 5:64–73. [PubMed: 14691482]
41. Ng L, et al. A thyroid hormone receptor that is required for the development of green cone photoreceptors. Nat Genet. 2001; 27:94–98. [PubMed: 11138006]

42. Bunting M, Bernstein KE, Greer JM, Capecchi MR, Thomas KR. Targeting genes for self-excision in the germ line. Genes Dev. 1999; 13:1524–1528. [PubMed: 10385621]

43. Kim DS, Matsuda T, Cepko CL. A core paired-type and POU homeodomain-containing transcription factor program drives retinal bipolar cell gene expression. J Neurosci. 2008; 28:7748–7764. [PubMed: 18667607]

44. Ng L, et al. Two transcription factors can direct three photoreceptor outcomes from rod precursor cells in mouse retinal development. J Neurosci. 2011; 31:11118–11125. [PubMed: 21813673]

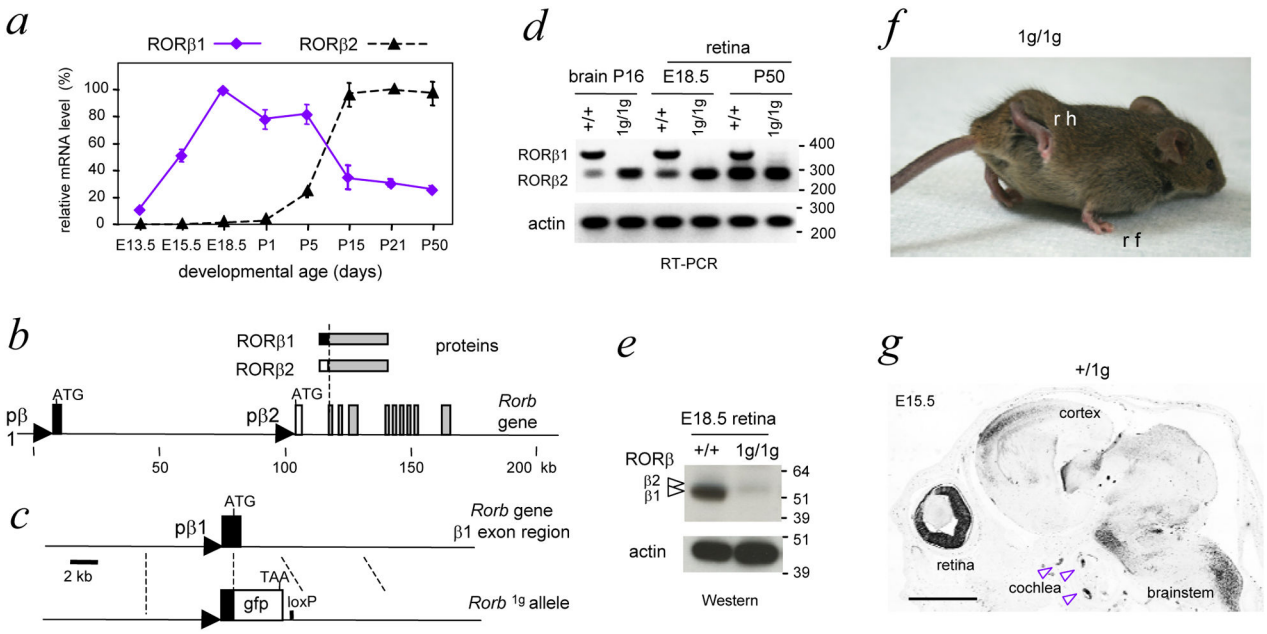

Figure 1. Differential expression of RORβ isoforms and targeted deletion of RORβ 1

a, RORβ1 and RORβ2 mRNA expression profiles in mouse retinal development, determined by qPCR analysis. Levels for each isoform are indicated as percentages relative to the highest level, assigned a value of 100%.

b, *Rorb* gene with RORβ1- and RORβ2-specific exons depicted as black and white boxes, respectively, common exons as grey boxes and RORβ1 and RORβ2 promoter regions as triangles.

c, Targeted replacement of the coding portion of the RORβ1-specific exon with a green fluorescent protein (gfp) cassette that carries a TAA translational stop codon. Excision of the neomycin-resistance ACN cassette left a residual loxP site in the *Rorb*^{1g} allele.

d, Loss of RORβ1 mRNA and retention of RORβ2 mRNA in brain and retina in 1g/1g mice shown by PCR with control analysis for β-actin. DNA size marker, bp.

e, Loss of RORβ1 protein in the retina in 1g/1g mice shown on a western blot with control analysis for β-actin. Arrowheads, bands for RORβ1 (lower, ~52 kDa) and RORβ2 (upper, ~53 kDa). The gfp protein expressed in 1g/1g mice carries no RORβ protein sequence and was detected with antibody against gfp as a ~27 kDa band (not shown). Protein molecular size marker, kDa.

f, Abnormal gait in 1g/1g mice with exaggerated lifting and clasping of hindlimbs; rh, right hindlimb; rf, right forelimb.

g, Para-sagittal section of +/1g embryonic head showing gfp expression in retina, cochlea and brain. Expression of gfp was detected by immunohistochemistry (dark areas). Scale bar, 1mm.

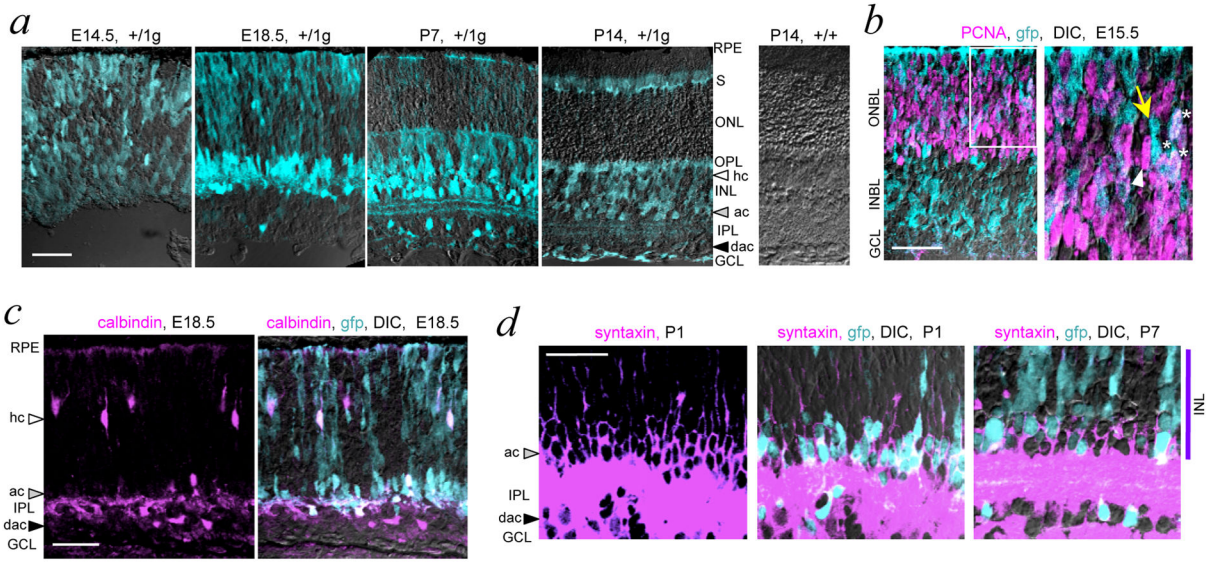

Figure 2. Expression of *Rorb*^{1g} allele in retina

a, Developmental analysis in +/1g mice showing gfp (turquoise fluorescence) overlaid on differential interference contrast (DIC) images to show cell layers. GCL, ganglion cell layer, INL, inner nuclear layer, IPL, inner plexiform layer, ONL, outer nuclear layer, OPL, outer plexiform layer, RPE, retinal pigmented epithelium, S, inner/outer segment layers. White, grey and black arrowheads indicate horizontal cell (hc), amacrine cell (ac) and displaced amacrine cell (dac) zones, respectively. Control +/+ retina shows absence of gfp signal. Scale bars, 30 μm in all panels.

b, Detection of proliferative progenitor cells (PCNA, purple) that express gfp (turquoise) overlaid on a DIC image in a +/1g embryo. Double detection of gfp and PCNA required HCl pre-treatment of sections. In the outer neuroblastic layer (ONBL), many cells co-express both PCNA and gfp (white or whitish). *Right*, enlargement of boxed ONBL area showing PCNA$^+$/gfp$^+$ cells (asterisks), PCNA$^+$ cells (white arrowhead) and gfp$^+$ cells (yellow arrow).

c, *Rorb*^{1g} expression (turquoise) in immature horizontal, amacrine and displaced amacrine cells identified with calbindin (purple) in a +/1g embryo. Co-localization of calbindin and gfp results in whitish cells, overlaid on a DIC image.

d, *Rorb*^{1g} expression (turquoise, soma) in immature amacrine cells identified with syntaxin (purple, honeycomb pattern around the soma). At P1 (*left two panels*), most syntaxin$^+$ cells are gfp$^+$ but at P7 (*right*), fewer are gfp+ and many have only weak gfp signals. Amacrine cells form a zone ~3 soma deep next to the INL.

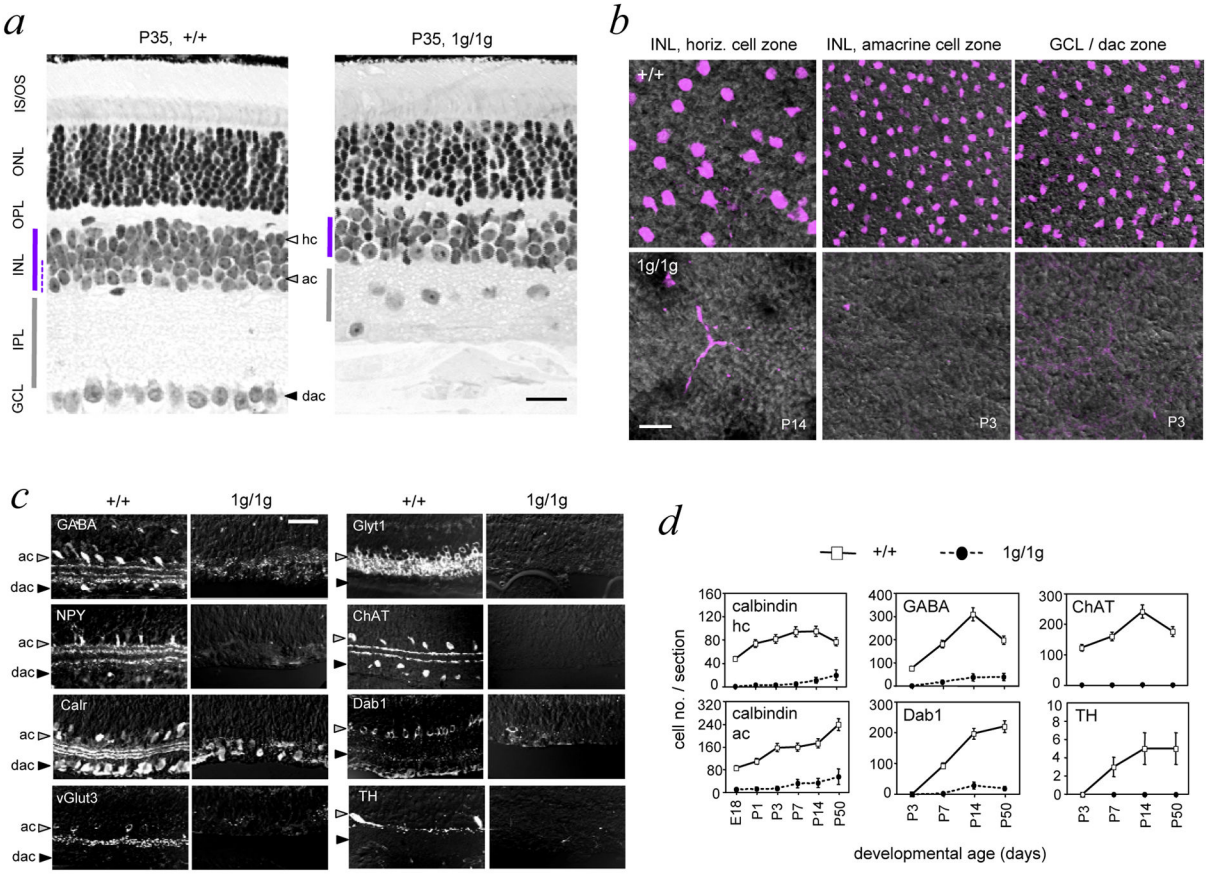

Figure 3. Loss of amacrine and horizontal cells in *Rorb*$^{1g/1g}$ mice

a, Histological sections showing disorganized inner plexiform, outer plexiform and ganglion cell layers in 1g/1g mice at P35. Note the thin INL (purple bar) and mis-located ganglion cell soma in the collapsed IPL in 1g/1g mice. Amacrine cell zone in the INL is indicated by a dashed line in +/+ retina. Scale bars, 30 μm in all panels.

b, Retinal flatmounts analyzed by confocal microscopy in the plane of horizontal (hc), amacrine (ac) and displaced amacrine (dac) cell zones using calbindin as a marker (purple) on DIC images to show tissue structure. Calbindin^{+} horizontal and amacrine cells are missing in 1g/1g mice.

c, Retinal sections showing loss of representative amacrine cell markers (GABA, GlyT1, NPY, ChAT, calretinin/calr, Dab1, vGlut3, TH) in 1g/1g mice at P14 (except NPY at P7).

d, Cell counts showing failure to generate amacrine and horizontal cells, identified with horizontal (calbindin/hc) and amacrine (calbindin/ac, GABA, ChAT, Dab1, TH) markers. Calbindin^{+} horizontal and amacrine cells were distinguished in +/+ mice by morphology and location in the INL. Cell counts, given as mean ± S.D., were based on analysis of 12 cryosections of the retina representing ≥ 3 mice at each age.

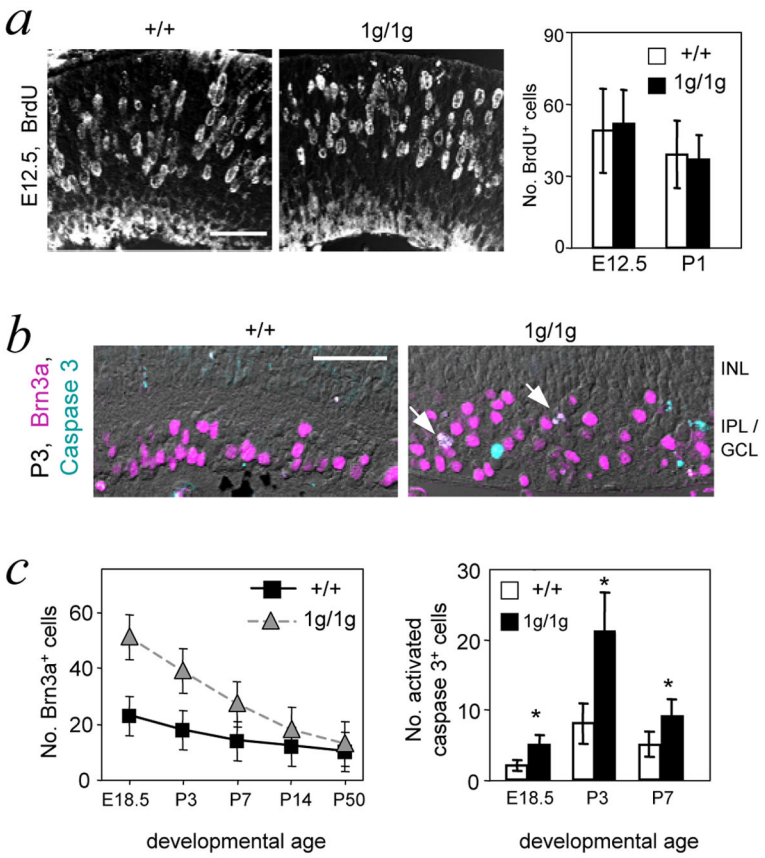

Figure 4. Excess ganglion cells in *Rorb*$^{1g/1g}$ mice

a, Normal numbers of BrdU^{+} proliferating cells were detected in the retina in 1g/1g mice 1 hour after a pulse delivery of BrdU. Graph of BrdU^{+} cell counts at E12.5 and P1 shows no differences between +/+ and 1g/1g mice; mean ± s.d.; p >0.8. Counts represent BrdU^{+} cells per 150 μm length of retina, determined on 10 μm thick cryosections. Scale bars, 30 μm in all panels.

b, Immunostaining for Brn3a^{+} ganglion cells (purple) in retinal sections at P3. Sections were co-stained for activated caspase 3 (turquoise), a marker of apoptotic cells. Arrows, double-labeled cells in 1g/1g mice, which were rarely observed in +/+ mice.

c, The postnatal decline in excess Brn3a^{+} cells correlated with increased cell death rates in 1g/1g mice. *Left*, counts of Brn3a^{+} cells per 150 μm length of retina in 10 μm thick sections. For +/+ and 1g/1g differences at E18.5, P3 and P7, p <0.001. *Right*, counts of caspase 3^{+} cells per section; mean ± s.d.; *, p< 0.001. Statistical analyses were performed using Student's t-test.

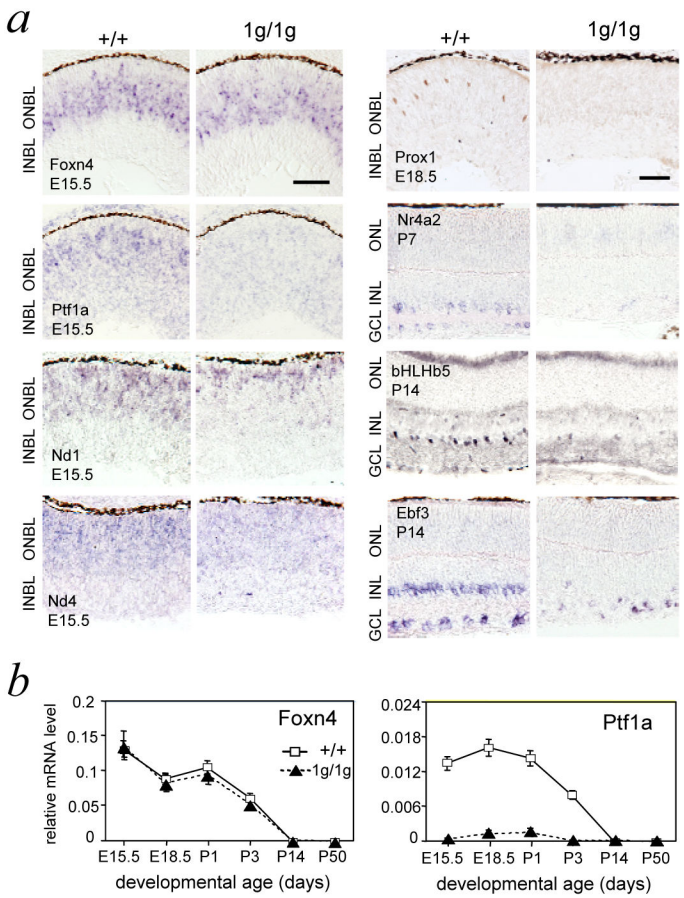

Figure 5. Expression of retinal transcription factors in *Rorb*$^{1g/1g}$ mice

a, Transcription factor expression analyzed by *in situ* hybridization (Foxn4, Ptf1a, Nd1, Nd4, Nr4a2, Ebf3) or immunohistochemistry (Prox1, bHLHb5), at stages when each factor normally displays prominent expression (early stages, *left*, or later maturation stages, *right*). Ptf1a was overtly and Nd1 and Nd4 were modestly reduced in 1g/1g mice. Expression of horizontal (Prox1) and amacrine sub-lineage (Nr4a2, bHLHb5, Ebf3) markers was severely reduced in 1g/1g mice. Scale bar, 30 μm.

b, Quantitative PCR analysis demonstrating normal *Foxn4* but reduced *Ptf1a* mRNA levels in *Rorb*$^{1g/1g}$ mice along development. Each point represents mean of 3 analyses on pooled retina (>4 mice) at each age. Plots based on mean ± S.D. at each age.

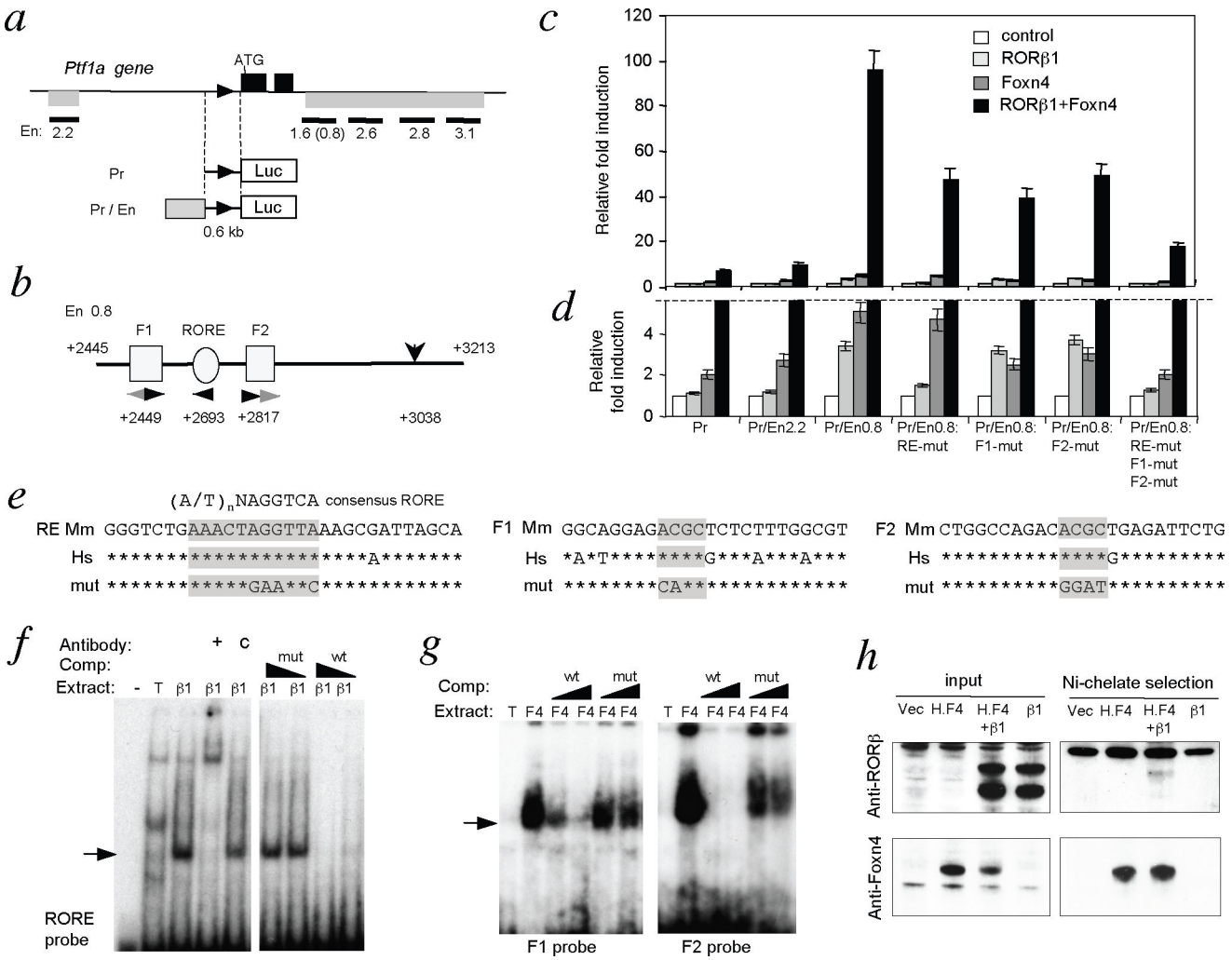

Figure 6. RORβ1-responsive enhancer in *Ptf1a* gene

a, *Ptf1a* gene; black boxes, exons; triangle, promoter; grey bars below gene, enhancer regions. Enhancer (En) fragments tested are shown as black bars with size (kb) below. Reporter constructs contained a 0.6 kb *Ptf1a* promoter driving luciferase without (Pr) or with enhancer fragments (Pr/En).

b, Foxn4 (F1, F2) and RORβ1 (RORE) response elements in En0.8 fragment. Arrowheads, motifs and orientation; black arrowheads, conserved between mouse and human genomes. Numbers, distances (in bp) from ATG. Vertical arrow (+3038) indicates a distant control mutation.

c, Luciferase assays in 293T cells for reporter responses to RORβ1 and Foxn4 normalized to basal expression of each reporter in absence of added factors; means ± s.d.. Pr/En0.8 gave >10-fold greater synergistic induction than Pr promoter alone ($p < 0.001$). Fold induction of Pr/En0.8 by both factors together (black columns) was reduced by individual or combined mutagenesis (mut) of RORE, F1 and F2 sites ($p < 0.001$ for each mutant compared to wild type). Statistical analyses were performed using Student's t-test.

d, Magnification of lower region of response scale in panel "c". *Note:* responses to both factors (black columns) are truncated above the dashed line.

e, RORE, F1 and F2 sequences in mouse (Mm) and human (Hs) genomes; asterisks indicate identity; core motifs shaded. Mouse wild type and mutant (mut) sequences were used as EMSA probes.

f, EMSA of RORβ1 binding to RORE using extracts from 293T cells transfected with RORβ1-expressing (β1) or empty (T) vector; probe alone (−). Competition with wild type (wt) but not mutant (mut) unlabeled oligonucleotides abolished the shifted band (arrow). Anti-RORβ antibody (+) but not IgG control (c) supershifted the band.

g, EMSA of Foxn4 binding to F1 and F2 using extracts from 293T cells transfected with Foxn4-expressing (F4) or empty (T) vector. Competition with wild type but not mutant oligonucleotides strongly diminished the shifted band (arrow).

h, Protein interaction between RORβ1 and Foxn4. *Left*, input protein from 293T cells transfected with empty vector (vec), or vectors expressing histidine-tagged Foxn4 (H.F4), RORβ1 (β1), or both (H.F4+β1) analyzed by western blot (RORβ, upper; Foxn4, lower). *Right*, Nickel-chelate selection for H.F4 protein co-selected a weak RORβ1 band. Protein molecular size marker, kDa.

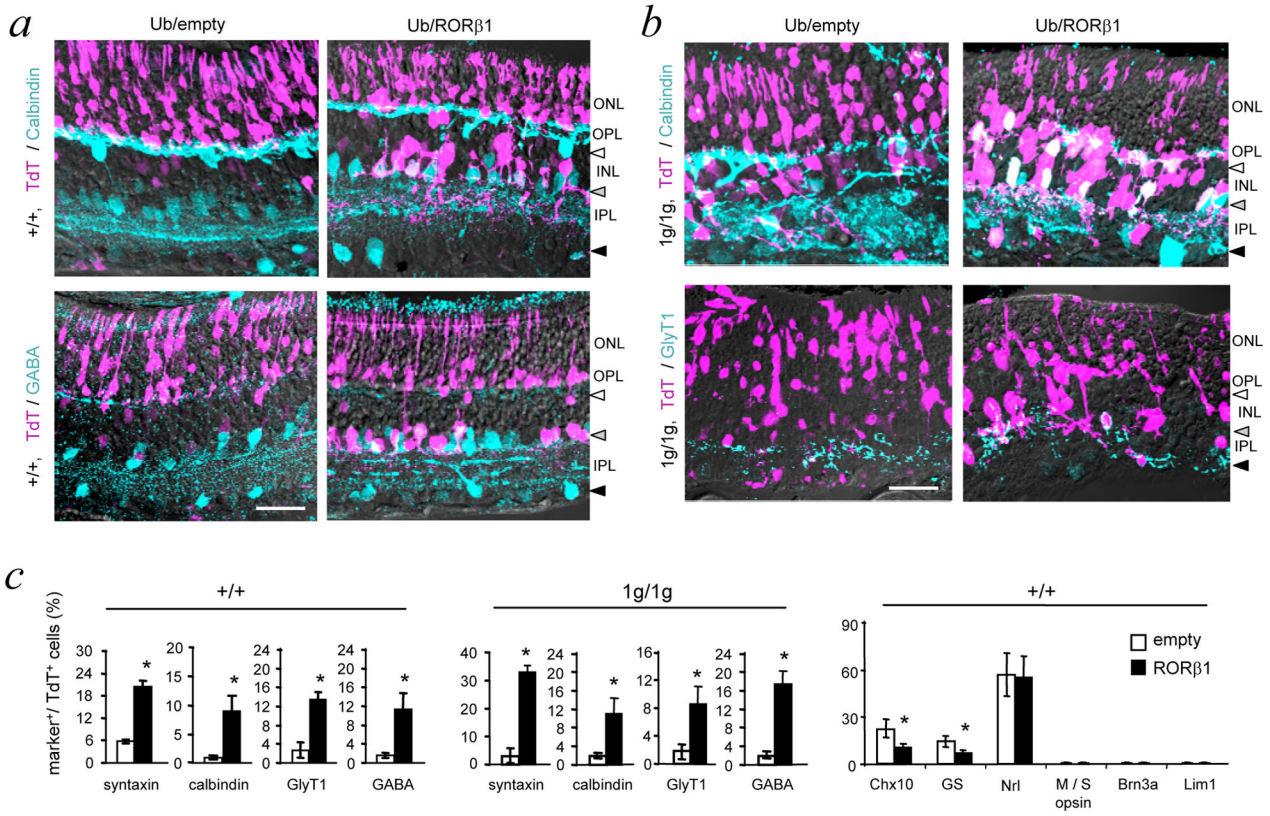

Figure 7. RORβ1 promotes amacrine cell differentiation

a, Retinal sections of +/+ mice at P14 after electroporation at P0 with Ub/empty control or Ub/RORβ1-expression vector. Electroporated cells were identified by co-electroporated TdT marker. TdT^+ (purple), $calbindin^+$ or $GABA^+$ amacrine cells (turquoise) and double-positive cells (white/whitish) were visualized by confocal imaging. Horizontal, amacrine and displaced amacrine cell zones are indicated by white, grey and black arrowheads, respectively. Ub/RORβ1 yielded many TdT^+ amacrine cells with projections in the inner plexiform layer. Scale bars, 30 μm in all panels.

b, In RORβ1-deficient (1g/1g) pups electroporated at P0 and analyzed at P14, Ub/RORβ1 yielded many TdT^+ amacrine-like cells in the INL with projections in the inner plexiform layer. TdT^+, $calbindin^+$ cells with unusual projections in the outer plexiform layer may be mis-located amacrine cells in the disorganized INL of 1g/1g mice.

c, Counts of cells positive for amacrine (syntaxin, GABA, GlyT1) and combined amacrine/horizontal (calbindin) markers in +/+ (*left*) and 1g/1g (*middle*) mice. Counts represent $marker^+/TdT^+$ electroporated cells in 150 μm lengths of retina. *Right*, counts in +/+ mice of cells positive for TdT and bipolar (Chx10), Muller glial (glutamine synthetase, GS), rod (Nrl), cone (M and S opsin), ganglion (Brn3a) or horizontal (Lim1) cell markers. Means ± s.d.; ≥6 eyes from ≥6 mice; *, $p < 0.001$. Statistical analyses were performed using Student's t-test.

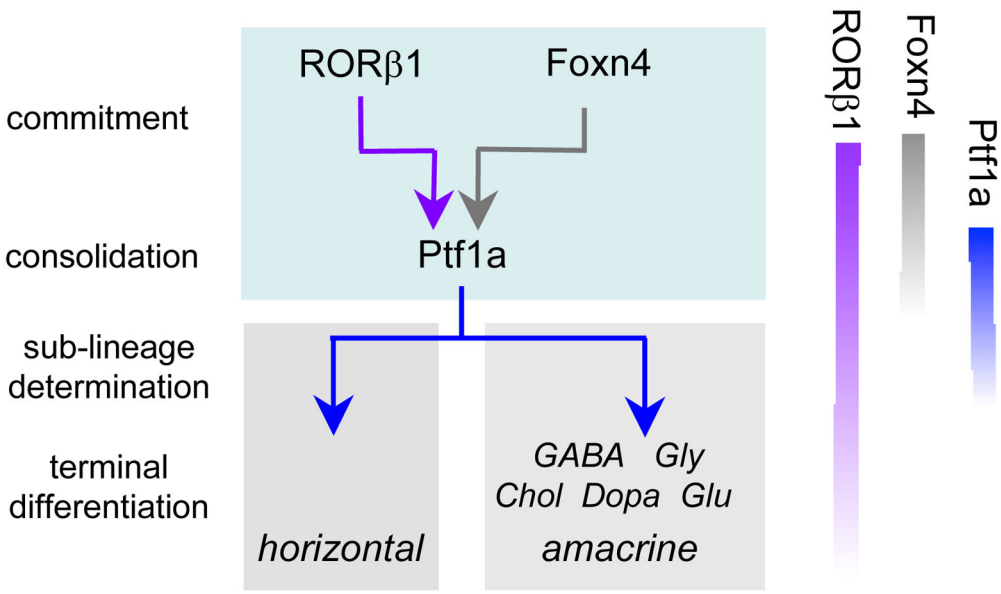

Figure 8. Proposed role for RORβ1 in amacrine and horizontal cell differentiation

It is proposed that RORβ1 and Foxn4 in progenitor cells cooperatively promote commitment to amacrine and horizontal cell fates by synergistic induction of Ptf1a. Ptf1a is transiently induced in post-mitotic precursors and consolidates the fates of both classes of interneurons. Many factors (not shown) contribute to the subsequent terminal differentiation of horizontal and amacrine cell sub-lineages, indicated here according to main neurotransmitter types (GABA, glycine, acetyl choline, dopamine, glutamate). Relative timing of expression of RORβ1, Foxn4 and Ptf1a is indicated on the right: Foxn4 is in dividing progenitors, Ptf1a in post-mitotic precursors and RORβ1 in both progenitors and precursors.